Available online at
https://jmeche.uitm.edu.my/

e-ISSN: 2550-164X

Journal of Mechanical Engineering 22(2) 2025,71 – 82.

Journal of Mechanical Engineering

Evaluation of Sliding Surfaces using Three-Dimensional Surface Texture Parameters

Keiichi Ninomiya[1*], Sho Yano[2], Shun Yoshida[1], Mizuho Nakamura[1], Akira Kakimoto[1]

[1]*Polytechnic University, Tokyo and Japan*
[2]*Wakayama Polytechnic Center, Wakayama and Japan*

ARTICLE INFO

Article history:
Received 19 July 2024
Revised 8 November 2024
Accepted 30 January 2025
Online first
Published 31 May 2022

Keywords:
Surface roughness
Surface texture
Design guidelines
Sliding surface

DOI:
https://doi.org/10.24191/jmeche.v22i2.6179

ABSTRACT

In mechanical drawings, two-dimensional surface texture parameters are commonly used to indicate surface texture; however, measurement results may vary depending on the measurement position. As a result, there is increasing interest in establishing a measurement method that utilizes three-dimensional surface quality parameters, which can more effectively evaluate fine surface irregularities. The application of three-dimensional evaluation is proposed as essential in the design of sliding surfaces for high-precision machined parts and overall machine design. This study emphasizes the need to clarify design guidelines and evaluation criteria when assessing products and designing machines. It aims to evaluate the impact of surface roughness on the friction and wear characteristics of reciprocating sliding surfaces, with a view to serving as a guideline for designing sliding surfaces under light load conditions. The experiment involved preparing three types of sliding surfaces - ground and milled - each with different surface roughness. Results indicate that the friction coefficient increases with sliding distance, demonstrating significant wear on the surface crests. Thus, it was found effective to use a combination of multiple surface quality parameters, such as the arithmetic mean peak curvature *Spc*, in addition to the arithmetic mean roughness *Ra*, for evaluating sliding surfaces. This finding is expected to enhance the product value by enabling more detailed evaluation of surface quality in the mechanical design of sliding surfaces.

INTRODUCTION

In recent years, as international competitiveness in the manufacturing industry has intensified, machine tools and industrial robots are increasingly required to provide added value through higher precision and longer service life. In response to these demands, advanced technologies such as laser machining and additive manufacturing have made significant progress alongside traditional cutting processes, driving

[1*] Corresponding author. *E-mail address*: ninomiya@uitec.ac.jp
https://doi.org/10.24191/jmeche.v22i2.6179

reforms in manufacturing practices (Rahmatullah et al., 2021; Adeleke et al., 2024; Fukuoka & Seiyama, 2020; Cooke et al., 2020; Hashimoto, 2022). Similarly, measurement technologies used for inspecting and evaluating machined parts now require a broader range of methods. For example, surface properties, which indicate the surface condition and characteristics of the measured object, are one such area requiring attention (Baršić et al., 2023; Zeng et al., 2018).

In general, the arithmetic mean roughness *Ra* and the maximum height roughness *Rz*, as specified in ISO standards, are commonly used to represent surface properties in mechanical drawings (ISO 25178-2, 2021). *Ra* and *Rz*, which quantitatively assess the degree of surface roughness, are widely adopted due to the global standardization of line evaluation using measured cross-sectional curves as a common industrial practice (Gadelmawla et al., 2002; Sasaki, 2014). However, as shown in Fig 1, although both surfaces have the same *Ra* and *Rz* values, the surface in Fig 1(a) is considered more susceptible to wear, while the surface in Fig 1(b) is considered more resistant to wear in terms of functional properties. Therefore, despite identical surface roughness specifications, differences in wear characteristics between the two surfaces remain a concern.

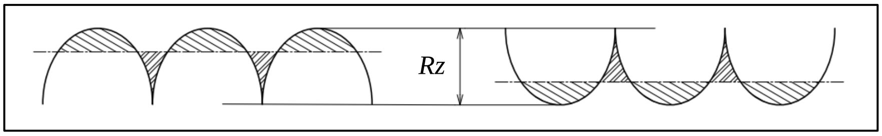

Fig. 1. Surfaces with the same roughness but different functionality (a) pattern1 and (b) pattern2.

The challenge in evaluating two-dimensional surface texture parameters lies in the fact that it essentially involves a line evaluation, where only a segment of the entire machined surface is represented as a straight line. Consequently, measurement outcomes can vary depending on the location of the measurement and the scanning direction. In contrast, three-dimensional surface property parameters, while providing a more comprehensive analysis, have their own drawbacks, such as lengthy measurement times and the vast data volume required to evaluate large surface areas. However, because this method evaluates the entire surface, it allows for the detection of striations and microscopic irregularities often missed by two-dimensional line evaluations, and it can assess surfaces specifically designed for functionality. Consequently, machine designers and machining engineers have high hopes for the development of a reliable evaluation method (He et al., 2021; Fu et al., 2020; Marrugo et al., 2020; Berglund et al., 2020).

Yonehara et al. (2003) investigated the effects of surface roughness on gloss and surface colour from a product quality perspective. Their results showed that as *Ra* decreased, gloss levels increased while surface colour diminished. Numerous studies on surface evaluation focus on texturing, which involves deliberately introducing fine irregularities to a surface. For example, Kyoizumi et al. (2018) improved the low friction coefficient and wear resistance of sliding surfaces by creating a microcavity and convexity profile using the plasma shot method, followed by grinding, and then evaluating the resulting shape and frictional wear. Their findings indicated that the friction coefficient decreased as the surface roughness from grinding was reduced.

While many studies have focused on appearance, texture, and texturing of products as evaluation criteria for surface properties, there is a lack of comprehensive proposals and evaluations based on experimental data that serve as design guidelines for sliding surfaces (Sun et al., 2005; Gachot et al., 2017; Mao et al., 2020; Pawlus et al., 2021; Yonehara et al., 2005). Therefore, the purpose of this study is to evaluate the effects of three-dimensional surface property parameters on the friction and wear characteristics of reciprocating sliding surfaces, providing guidelines for designing these surfaces under

https://doi.org/10.24191/jmeche.v22i2.6179

light load conditions. Furthermore, based on the findings, we propose surface texture parameters that can aid in the design of sliding surfaces.

EXPERIMENTAL METHOD

Fig 2 shows a schematic diagram of the sliding device used in this experiment. The apparatus consists of a driving unit on the left side and a driven unit on the right side, both performing reciprocating motions. The load on the test specimen is adjusted by varying the thickness of the upper and lower test pieces. The friction coefficient Fy/Fz during sliding was calculated from the measured values of Fy and Fz, obtained using a dynamometer when the test pieces were positioned near the centre, with the sliding direction along the $-y$ axis. Additionally, frictional wear during sliding was monitored using a broadband AE sensor (Borghesani et al., 2018), installed at the midpoint of the side of the lower specimen. Since the AE signal generated during sliding is weak, data were acquired with a total gain of 70 dB, a high-pass filter set at 100 kHz, and a sampling frequency of 8 MHz.

Table 1 presents the main experimental conditions. Prior to sliding, an average load of 150 N was applied in the z direction, with a sliding speed of 10 mm/s. The contact area between the upper and lower specimens was 46 × 46 mm. The test material used was S50C, a carbon steel for mechanical structures. The upper specimen was ground to a surface roughness of $Ra \cong 0.2$ μm and a hardness of 227 HV (hereafter referred to as the untreated upper specimen). Another upper specimen was hard chrome plated to a roughness of $Ra \cong 0.2$ μm and a hardness of 808 HV (hereafter referred to as the hard chrome-plated upper specimen). The lower specimens were milled after grinding to achieve three different roughness levels: $Ra \cong 1.6$ µm, $Ra \cong 3.2$ µm, and $Ra \cong 6.3$ µm (referred to as $Ra \cong 1.6$ μm, $Ra \cong 3.2$ μm, and $Ra \cong 6.3$ μm, respectively). The sliding direction corresponded to the cutting direction of the specimens. Here, the sliding direction refers to the direction of motion in the device shown in Fig 2, while the cutting direction refers to the grinding direction on the surface and the tool feed direction during milling. A thin layer of lubricating oil was applied to the contact surfaces of the upper and lower specimens before starting the experiment. Since the aim of this study was to evaluate the effect of surface roughness on wear and friction characteristics, the experiments were conducted under lubricated wear conditions, with lubricant applied only at the start of sliding. Subsequently, the experiments simulated a wear state in which the lubricant had disappeared from the sliding surfaces. The experiment was repeated five times to ensure reproducibility, confirming that the relationship between sliding distance and friction coefficient was qualitatively consistent.

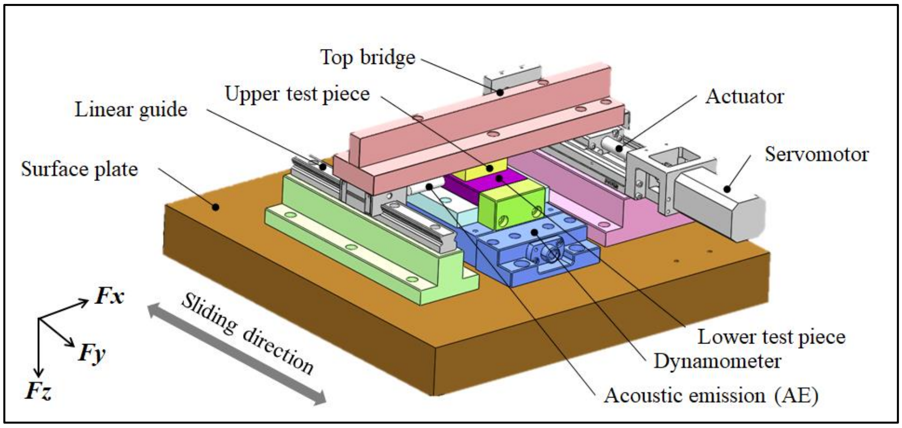

Fig. 2. Schematic diagram of the experimental setup.

https://doi.org/10.24191/jmeche.v22i2.6179

Table 1. Experimental conditions

Upper test piece	S50C Ground surface (*Ra* ≅ 0.2 μm) Hard chrome-plated (808 HV)		 Untreated (227 HV)
Lower test piece	S50C Milled surface (227 HV) *Ra* ≅ 1.6 μm	 *Ra* ≅ 3.2 μm	 *Ra* ≅ 6.3 μm
Speed	10 mm/s		
Load	150 N (7.2 × 10^{-3} MPa)		
Contact area	46 × 46 mm		
Lubrication oil	VG-68 (50 μl)		

Table 2. Measurement conditions of the laser microscope

Microscope	KeyenceVK-X1000	
Lens	× 20	
Condition	S-filter 2 μm	L-filter 0.5 mm
Area	500 × 500 μm	
Pixel	1024×768	

The surface of the test piece undergoes noticeable changes before and after sliding due to abrasion. This abrasion affects both the friction coefficient and the surface appearance. To assess these changes, we measured the static friction coefficient, dynamic friction coefficient, and glossiness before and after sliding. Additionally, a non-contact laser microscope was used to observe the specimen and to measure surface texture parameters before and after sliding. The main measurement conditions for the microscope are listed in Table 2. It was operated at a magnification of 20x, and surface texture parameters were calculated over an area of 500 × 500 μm.

EXPERIMENTAL RESULTS AND DISCUSSION

Correlation between Sliding Distance, Friction Coefficient, and Arithmetic Mean Roughness

Fig 3 illustrates the relationship between sliding distance, friction coefficient, and arithmetic mean roughness. In Fig 3(a), the lower test piece has an *Ra* ≅ 1.6 μm, and in Fig 3(b), it has an *Ra* ≅ 6.3 μm. The results show that the friction coefficient follows a similar increasing trend, regardless of the surface roughness and hardness of the test piece. In Fig 3(a), for the upper plated surface, the friction coefficient remains low from the beginning of sliding until around 80 m, after which it increases compared to the upper ground surface. It is believed that when the upper surface is plated, the crests of the lower specimen wear more readily than on a ground surface, leading to a rise in the friction coefficient. This occurs due to a reduction in chip pockets as wear progresses, which diminishes the retention and discharge function of wear debris. This finding aligns with the abrasive wear observations by Nitanai (2000), who reported that when there is a hardness disparity between two contacting surfaces, the rough projections of the harder material penetrate the softer one, cutting into it and forming grooves through relative movement. Conversely, in Fig 3(b), the friction coefficient is lower than that observed in the sliding test with the upper ground surface, up to a sliding distance of about 230 m. Brunetière & Tournerie (2012) reported that introducing dimples to metal surfaces in contact can reduce friction. Consistent with this, the experimental results suggest that, due to the large ridges, the chip pocket function is effective even as wear occurs, resulting in a lower friction coefficient (Sedlacek et al., 2009; Kakegawa et al., 2015). Furthermore, no significant change in *Ra* was observed before and after sliding for both the upper ground and upper plated surfaces.

https://doi.org/10.24191/jmeche.v22i2.6179

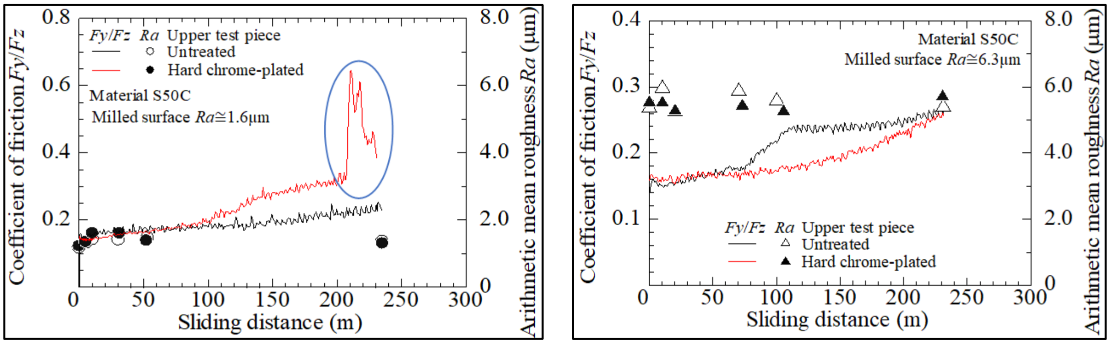

(a) (b)

Fig. 3. Relationship between sliding distance, friction coefficient, and arithmetic mean roughness (a) lower specimen milled surface *Ra* ≅ 1.6 μm and (b) lower specimen milled surface *Ra* ≅ 6.3 μm.

Fig 4 shows the measured cross-sectional curve. In Fig 4(a), the lower test piece has an *Ra* ≅ 1.6 μm, and in Fig 4(b), it has an *Ra* ≅ 6.3 μm. Additionally, images of the lower test piece (*Ra* ≅ 6.3 μm) before and after sliding are presented in Fig 5. In Fig 5(a), the upper test piece is untreated, while in Fig 5(b), it is hard chrome-plated. These results indicate that the surface peaks were worn down before and after sliding. For the upper ground part, particularly in the case of the ground surface, as the sliding distance increased shortly after the start of sliding, the surface convexities experienced plastic deformation and were gradually worn away, creating a wear surface. This process increased the friction coefficient. Once the wear surface was fully established and the real contact area increased, the contact pressure from the applied load decreased, which reduced the deformation of the convexities and stabilised the friction coefficient (Gachot et al., 2017; Nogueira et al., 2002). Furthermore, in cases where the friction coefficient rose again after stabilization, it is likely that the lubricating effect weakened due to wear debris causing adhesion on the sliding surfaces (Miyoshi & Tsukamoto, 2023; Pettersson & Jacobson, 2004). The sharp rise in the friction coefficient, highlighted by the blue circle on the upper plated surface in Fig 3(a), is likely due to valleys acting as pseudo oil pockets. These pockets initially expel lubricant along with wear debris, but as the effectiveness of the lubricant diminishes, scratches form on the sliding surface. This can be observed from the sliding marks on the side of the test piece in the photograph taken immediately after sliding, as shown in Fig 6. Additionally, when comparing *Sz* values before and after sliding, area B had a maximum height *Sz* of 7.969 μm before sliding and 7.323 μm after sliding, while area A had an *Sz* of 7.322 μm before sliding and 9.061 μm after. Experiments conducted under non-lubricated conditions confirmed that with larger *Ra* values, wear debris took a longer distance to become trapped, demonstrating the effect of chip pockets in the valleys.

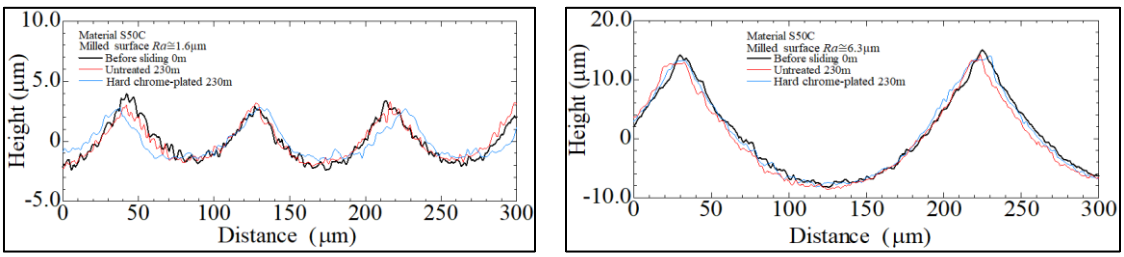

(a) (b)

Fig. 4. Measurement cross-section curve (a) lower specimen milled surface *Ra* ≅ 1.6 μm and (b) lower specimen milled surface *Ra* ≅ 6.3 μm.

https://doi.org/10.24191/jmeche.v22i2.6179

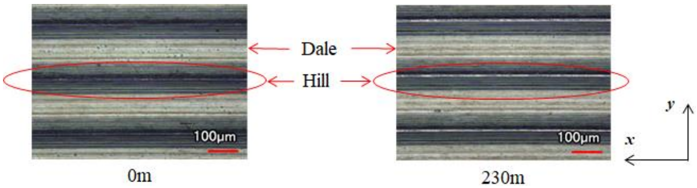

(a)

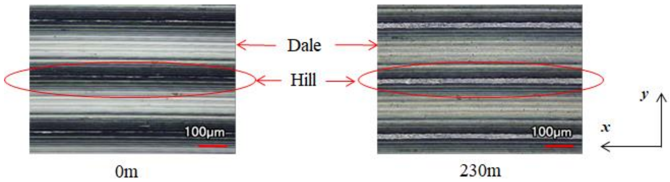

(b)

Fig. 5. Images of the lower test piece *Ra* ≅ 6.3 µm before and after sliding (a) upper untreated and (b) upper hard chrome-plated.

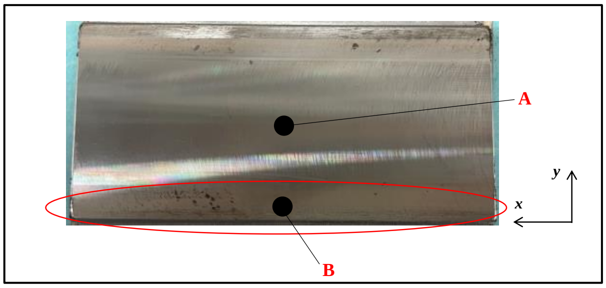

Fig. 6. An example image of the lower test piece with *Ra* ≅ 1.6 µm (The upper test piece is hard chrome-plated).

Fig 7 illustrates the relationship between sliding distance, glossiness, and arithmetic mean roughness on the upper plated surface. The results indicate that as the sliding distance increases, glossiness slightly improves from its initial level, regardless of surface roughness. This improvement is likely due to surface peaks being worn down during sliding, which increases the amount of specularly reflected light (Yonehara et al., 2003; Yonehara et al., 2005). However, since the change in *Ra* due to sliding is minimal, evaluating the surface condition based solely on gloss remains challenging.

Relationship between Sliding Distance and Arithmetic Mean Curvature of the Peak

From the measured cross-sectional curve shown in Fig 4, it is inferred that changes in the friction coefficient are partly influenced by alterations in the shape of the surface peaks. Accordingly, Fig 8 presents a bird's-eye view of the lower surface with *Ra* ≅ 6.3 µm. Fig 8(a) illustrates the surface before sliding, Fig 8(b) shows the surface after a sliding distance of 230 m for the untreated material, and Fig 8(c) depicts the surface after a sliding distance of 230 m following a hard chrome-plating treatment. In the figure, red represents the highest points, while blue represents the lowest points. The results indicate that, as sliding distance increases, the peaks of the surface gradually wear down.

https://doi.org/10.24191/jmeche.v22i2.6179

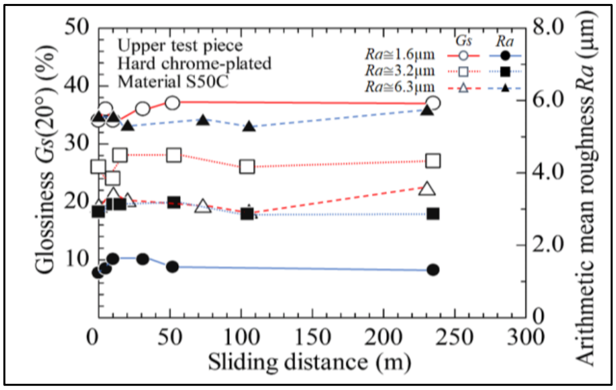

Fig. 7. Relationship between sliding distance, glossiness and arithmetic mean roughness.

Next, we used the arithmetic mean peak curvature *Spc* at the summit point as a three-dimensional surface property parameter to evaluate the shape of the peaks. The *Spc* peak identification method was set to 5% of the maximum amplitude at the contour surface. *Spc* reflects the sharpness of the contact points, with smaller values indicating more rounded peaks (ISO 25178-2, 2021). Fig 9 illustrates the relationship between sliding distance, *Spc,* and the acoustic emission AE effective value. The results show that the AE effective value is higher immediately after the start of sliding compared to other measurement points. This is because the initial surface has sharp peaks that undergo significant wear during sliding. Additionally, the AE effective value is higher on the upper plated surface than on the upper ground surface. This difference is attributed to the varying hardness between the upper and lower specimens in the case of the upper plated surface, causing the lower specimen to wear more rapidly. This suggests that softer surfaces experience greater wear compared to harder surfaces (Suzuki et al., 2008; Kikuchi et al., 1998).

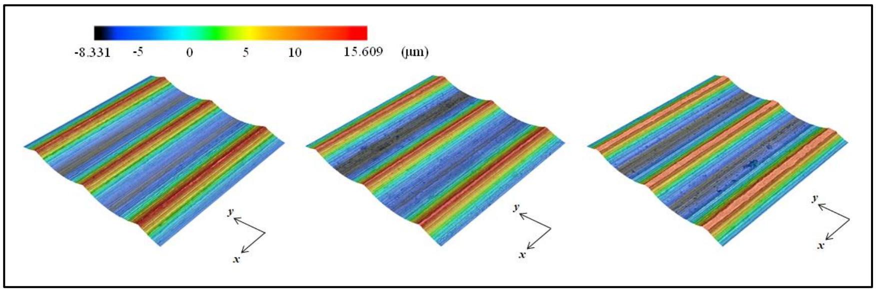

(a) (b) (c)

Fig. 8. Bird's eye view, lower specimen milled surface *Ra* ≅ 6.3 µm (500 × 500 µm) (a) before sliding 0 m, (b) untreated 230 m, and (c) hard chrome-plated 230 m.

https://doi.org/10.24191/jmeche.v22i2.6179

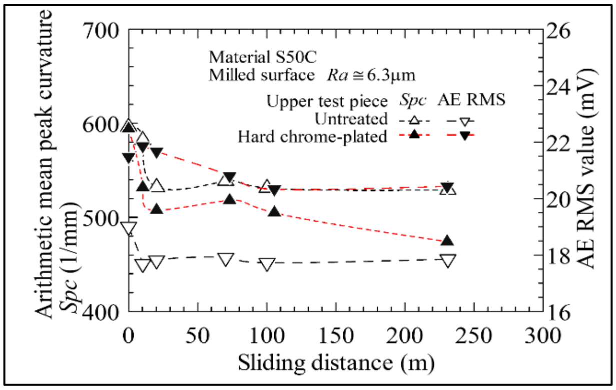

Fig. 9. Relationship between sliding distance, arithmetic mean curvature of mountain peak and AE effective value.

Relationship between Sliding Distance and Protruding Peak Height/Protruding Valley Depth

In a sliding experiment with the upper plated surface, the *Spc* value indicated that the shape of the peaks changed due to sliding. A similar trend was observed in the sliding experiment with the upper ground surface. At this point, a high effective AE value suggested that only the softer lower specimen was subjected to wear. Therefore, the surface of the lower test piece, before and after sliding with the upper plated surface, was characterized using load curve parameters: reduced peak height *Spk* and reduced valley depth *Svk*: (ISO 25178-2, 2021).

If the roughness curve is symmetrical about the centre line, then *Spk*/*Svk* = 1. An increase in this ratio compared to the pre-sliding condition indicates a significant change in the peaks, while a decrease suggests a smaller change. Fig 10 illustrates the relationship between sliding distance, *Spk*/*Svk*, and the friction coefficient. The results show that *Spk*/*Svk* increased immediately after the start of sliding and then gradually converged. This increase likely occurred because the initial sliding phase scraped away the protruding peaks. As wear continued, the peaks were gradually milled down, creating a surface where the tops of the peaks were removed, thus increasing the contact area. Consequently, *Spk*/*Svk* converged, and the friction coefficient rose. In summary, *Spk*/*Svk* serves as an effective parameter for evaluating the friction coefficient during sliding when there is a hardness difference between the contacting surfaces (Malkorra et al., 2020; Dzierwa, 2017).

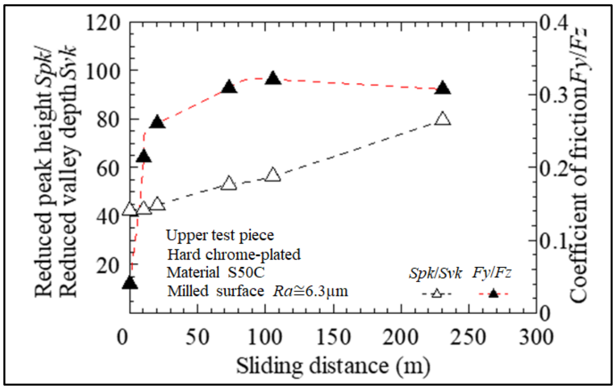

Fig. 10. Relationship between sliding distance, protruding peak height/protruding valley depth, and friction coefficient.

https://doi.org/10.24191/jmeche.v22i2.6179

Proposal of Design Guidelines for Sliding Surfaces

The combined use of the two-dimensional surface texture parameter *Ra* and the three-dimensional surface texture parameters *Spc, Spk*, and *Svk* has proven effective for evaluating sliding surfaces. Consequently, a radar chart was developed to serve as a technical reference for designing sliding surfaces, incorporating factors such as hardness, surface property parameters, friction coefficient, and gloss. Fig 11 illustrates this radar chart. The values for each factor were obtained at a sliding distance of approximately 230 m, with the hardness of the sliding surface expressed as the hardness ratio between the upper and lower test pieces. The results indicate that the friction coefficient and surface property parameters after sliding can be determined by establishing *Ra* and the hardness ratio of the upper and lower specimens, thereby providing processing guidelines. For instance, roughening the sliding surface increases nearly all surface texture parameters. At this stage, the friction coefficient is lowest at *Ra* ≅ 3.2 μm, indicating a correlation between the friction coefficient and *Spc*. Designers can use radar charts as technical references during sliding surface design to identify optimal parameters that align with the required specifications.

Furthermore, specifying surface properties with a single parameter can be challenging, as surface irregularities result from multiple surface characteristics. Therefore, in practical drawing instructions, it is advisable to include several parameters related to the required functions of the product, in addition to the conventional *Ra*.

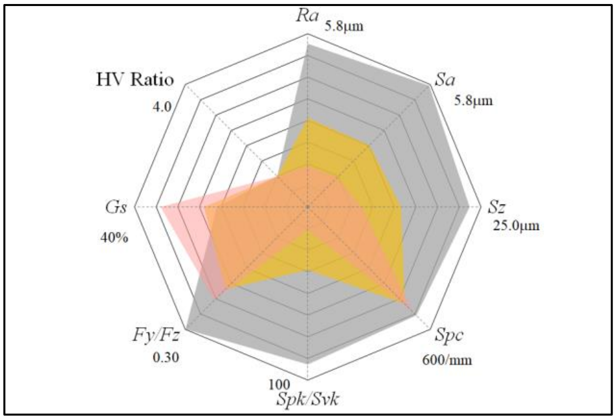

Fig. 11. Radar chart of surface texture parameters for untreated surfaces when surface roughness is specified.

CONCLUSION

As a guideline for designing sliding surfaces, we utilized an experimental device that simulates the sliding components to evaluate the surface roughness of ferrous metals and the influence of surface texture parameters on friction and wear characteristics. Additionally, we examined the effects of surface hardness on the friction coefficient during sliding, as well as the surface texture parameters before and after sliding. The findings are summarised below.

(i) When sliding between untreated ground and milled surfaces, as well as between ground and milled surfaces treated with hard chrome-plating, the coefficient of friction increased with increasing sliding distance, irrespective of the hardness of the upper specimen and the roughness of the lower specimen before sliding. In contrast, there was minimal change in the arithmetic mean roughness *Ra*. This suggests that three-dimensional surface parameters may

https://doi.org/10.24191/jmeche.v22i2.6179

offer a more effective evaluation of friction and wear compared to traditional two-dimensional surface parameters.

(ii) The shape of the crest of the lower specimen changes with sliding distance due to wear. Effective factors for evaluating the coefficient of friction during sliding include the arithmetic mean peak curvature *Spc* of the crest, along with the reduced peak height/reduced valley depth *Spk*/*Svk* when used in combination. Therefore, design guidelines should integrate *Ra* with three-dimensional parameters to achieve optimal surface texture.

(iii) A radar chart was created to serve as a guideline for the design of sliding surfaces. The results indicate that a combination of *Ra*, which provides a guideline for machining, and a factor that offers detailed instructions for the uneven shape is necessary for fabricating sliding surfaces that minimize the increase in the coefficient of friction.

ACKNOWLEDGEMENTS/ FUNDING

The authors would like to thank the students and Polytechnic University for their cooperation in this study and for facilitating access to laboratory facilities. This work did not receive any specific grant from funding agencies.

CONFLICT OF INTEREST STATEMENT

The authors agree that this research was conducted in the absence of any self-benefits, commercial or financial conflicts, and declare the absence of conflicting interests with the funders.

AUTHORS' CONTRIBUTIONS

The authors confirm their contribution to the paper as follows: study conception and design: Keiichi Ninomiya, Shun Yoshida, Mizuho Nakamura, Akira Kakimoto; data collection: Sho Yano; analysis and interpretation of results: Keiichi Ninomiya, Shun Yoshida, Sho Yano; draft manuscript preparation: Keiichi Ninomiya, Shun Yoshida, Sho Yano, Mizuho Nakamura, Akira Kakimoto. All authors reviewed the results and approved the final version of the manuscript.

REFERENCES

Adeleke, A. K., Montero, D. J. P., Ani, E. C., Olu-lawal, K. A., & Olajiga, O. K. (2024). Advances in ultraprecision diamond turning: Techniques, applications and future trend. Engineering Science & Technology Journal, 5(3), 740-749.

Baršić, G., Nujić, B., & Šimunović, V. (2024). Accuracy of replication of surface texture with a contact profile method. Materials and Technology, 58(1), 41-46.

Berglund, J., Söderberg, R., Wärmefjord, K., Leach, R., & Morse, E. (2020). Functional tolerancing of surface texture - a review of existing methods. Procedia CIRP, 92, 230-235.

Borghesani, P., Smith, W. A., Zhang, X., Feng, P., Antoni, J., & Peng, Z. (2018). A new statistical model for acoustic emission signals generated from sliding contact in machine elements. Tribology International, 127, 412-419.

https://doi.org/10.24191/jmeche.v22i2.6179

Brunetière, N., & Tournerie, B. (2012). Numerical analysis of a surface-textured mechanical seal operating in mixed lubrication regime. Tribology International, 49, 80-89.

Cooke, S., Ahmadi, K., Willerth, S., & Herring, R. (2020). Metal additive manufacturing: Technology, metallurgy and modelling. Journal of Manufacturing Processes, 57, 978-1003.

Dzierwa, A. (2017). Influence of surface preparation on surface topography and tribological behaviours. Archives of Civil and Mechanical Engineering, 17(3), 502-510.

Fu, S., Kor, W. S., Cheng, F., & Seah, L. K. (2020). In-situ measurement of surface roughness using chromatic confocal sensor. Procedia CIRP, 94, 780-784.

Fukuoka, Y., & Seiyama, T. (2020). Laser processing of robot system. Journal of Japan Laser Processing Society, 27(1), 22-27.

Gachot, C., Rosenkranz, A., Hsu, S. M., & Costa, H. L. (2017). A critical assessment of surface texturing for friction and wear improvement. Wear, 372-373, 21-41.

Gadelmawla, E. S., Koura, M. M., Maksoud, T. M. A., Elewa, I. M., & Soliman, H. H. (2002). Roughness parameters. Journal of Materials Processing Technology, 123(1), 133-145.

Hashimoto, T. (2022). Features and possibilities of latest 3D printing. Journal of Japan Institute of Light Metals, 72(10), 613-617.

He, B., Ding, S., & Shi, Z. (2021). A comparison between profile and areal surface roughness parameters. Metrology and Measurement Systems, 28(3), 413-438.

International Organization for Standardization. (2021). Geometrical product specifications (GPS) -Surface texture: areal. Part 2: terms, definitions and surface texture parameters (ISO 25178-2: 2021).

Kakegawa, T., Shimizu, T., Sagisaka, Y., & Yang, M. (2015). Surface texturing on micro-die and in-situ observation of its dry friction and wear behavior. Journal of the Japan Society for Technology of Plasticity, 56(657), 891-896.

Kikuchi, K., Kamiya, O., Saito, Y., & Kumagai, K. (1998). Running-in behavior of repeated dry wear on metals. Journal of the Society of Materials Engineering for Resources of Japan, 11(2), 12-20.

Kyoizumi, T., Egawa, A., Shibata, Y., Kato, C., Sumi, N., Shimada, K., Mizutani, M., & Kuriyagawa, T. (2018). Low wear / low friction interface generation by plasma-shot treatment and grinding processing. Journal of the Japan Society of Abrasive Technology, 62(7), 371-376.

Malkorra, I., Salvatore, F., Rech, J., Arrazola, P., Tardelli, J., & Mathis, A. (2020). Influence of lubrication condition on the surface integrity induced during drag finishing. Procedia CIRP, 87, 245-250.

Mao, B., Siddaiah, A., Liao, Y., & Menezes, P. L. (2020). Laser surface texturing and related techniques for enhancing tribological performance of engineering materials: a review. Journal of Manufacturing Processes, 53, 153-173.

Marrugo, A. G., Gao, F., & Zhang, S. (2020). State-of-the-art active optical techniques for three-dimensional surface metrology: a review. Journal of the Optical Society of America A, 37(9), B60-B77.

Miyoshi, R., & Tsukamoto, G. (2024). In-situ observation of sliding interface in commercially pure titanium sheet with a TiO2 film. Journal of the Iron and Steel Institute of Japan, 64(12), 1804-1812.

Nitanai, A. (2000). Tribology (friction and wear). Material Life, 12(2), 75-78.

https://doi.org/10.24191/jmeche.v22i2.6179

Nogueira, I., Dias, A. M., Gras, R., & Progri, R. (2002). An experimental model for mixed friction during running-in. Wear, 253, 541-549.

Pawlus, P., Reizer, R., & Wieczorowski, M. (2021). Functional importance of surface texture parameters. Materials, 14(18), 5326.

Pettersson, U., & Jacobson, S. (2004). Friction and wear properties of micro textured DLC coated surfaces in boundary lubricated sliding. Tribology Letters, 17, 553-559.

Rahmatullah, Amiruddin, A., & Lubis, S. (2021). Effectiveness of CNC turning and CNC milling in machining process. International Journal of Economic Technology and Social Sciences, 2(2), 575-583.

Sasaki, S. (2014). Surface texturing for improvement of tribological properties. Journal of the Surface Finishing Society of Japan, 65(12), 568-572.

Sedlacek, M., Podgornik, B., & Vizintin. J. (2009). Influence of surface preparation on roughness parameters, friction and wear. Wear, 266(3-4), 482-487.

Sun, J., Wood, R. J. K., Wang, L., Care, I., & Powrie, H. E. G. (2005). Wear monitoring of bearing steel using electrostatic and acoustic emission techniques. Wear, 259(7-12), 1482-1489.

Suzuki, K., Akebono, H., & Suzuki, H. (2008). The control of friction coefficient of DLC coatings using micro-dimpled substrate. Journal of the Surface Finishing Society of Japan, 59(9), 621-626.

Yonehara, M., Kihara, K., Isono, H., Sugibayashi, T., & Igata, N. (2005). Effect of surface roughness on glossiness and surface color for pure titanium and titanium nitride-coating surfaces. Journal of Japan Institute of Light Metals, 55(12), 668-672.

Yonehara, M., Suzuki, K., Kihara, K., Kijima, A., Isono, H., & Sugibayashi, T. (2003). Effect of surface roughness on glossiness of a 5052 aluminum alloy. Journal of Japan Institute of Light Metals, 53(4), 163-168.

Zeng, Q., Qin, Y., Chang, W., & Luo, X. (2018). Correlating and evaluating the functionality-related properties with surface texture parameters and specific characteristics of machined components. International Journal of Mechanical Sciences, 149, 62-72.

https://doi.org/10.24191/jmeche.v22i2.6179